



Cite this: *Chem. Commun.*, 2015, 51, 3854

Received 19th December 2014,  
Accepted 27th January 2015

DOI: 10.1039/c4cc10169c

[www.rsc.org/chemcomm](http://www.rsc.org/chemcomm)

## Doubly crosslinked microgel-colloidosomes: a versatile method for pH-responsive capsule assembly using microgels as macro-crosslinkers†

Wenkai Wang, Amir. H. Milani, Louise Carney, Junfeng Yan, Zhengxing Cui, Sineenat Thaiboonrod and Brian R. Saunders\*

**A new family of pH-responsive microgel-colloidosomes was prepared using microgel particles as the building blocks and macro-crosslinker. Our simple and versatile method used covalent inter-linking of vinyl-functionalised microgel particles adsorbed to oil droplets to form shells of doubly crosslinked microgels (DX MGs) and was demonstrated using two different microgel types.**

Hollow particles have been the focus of considerable attention in the literature because of their wide range of potential applications, which include pharmaceuticals, cosmetics, food, insulation and agriculture.<sup>1–3</sup> Furthermore, hollow particles offer unique functionalisation opportunities that may provide new tissue scaffolds and delivery methods for biologically active agents (cells, proteins, vitamins).<sup>4</sup> The most common approach for constructing hollow particles involves formation of the shell using pre-formed linear polymers,<sup>5,6</sup> which results in uniform shells on the colloidal length scale (*i.e.*, ~10 nm to 10 µm). It is becoming increasingly clear that the ability to provide textured surfaces on the colloidal length scale for hollow particles offers advantages in terms of facilitating surface–cell interactions<sup>4</sup> and the ability to selectively release nanometer-sized actives.<sup>7</sup> Here, we introduce a new method for constructing pH-responsive, surface textured, hollow particles that is simple, versatile and able to be performed using environmentally benign conditions (*i.e.*, aqueous solutions with temperature and pH values that, potentially, should not adversely affect biologic species such as cells or proteins).

Colloidosomes are micrometer-sized hollow particles that have shells consisting of coagulated or fused colloid particles<sup>3</sup> and were first reported by Velev *et al.*<sup>8</sup> The term colloidosome was later introduced by Dinsmore *et al.*<sup>9</sup> Most colloidosomes reported are non-responsive with built-in pore sizes that cannot be changed. This limitation results from their construction using hard particles. To overcome this performance constraint microgel particles

have been employed to prepare stimulus-responsive microgel-colloidosomes.<sup>10,11</sup> Microgels are crosslinked polymer particles that swell in a good solvent or when the pH approaches the  $pK_a$  of the constituent polymer.<sup>12</sup> One of the inherent advantages offered by microgel-colloidosomes is that the pore size within the shells can be tuned using environmental response (*e.g.*, pH<sup>11</sup>) which enables triggered release for encapsulated actives. Furthermore, because microgel particles can themselves exhibit triggered release of actives,<sup>13</sup> microgel-colloidosomes could provide opportunity for a hierarchical release system. The surface properties of microgel-colloidosomes (*e.g.*, texture and hydrophobicity) depend on the microgel particles which can, in turn, be designed to enable reversible adsorption and detachment of cells.<sup>14</sup> Consequently, microgel-colloidosomes have excellent potential for delivery, cell harvesting and responsive tissue scaffolds. Progress towards achieving these goals will benefit from microgel-colloidosome preparation methods that use environmentally benign conditions and a minimal number of building blocks (preferable only one). These design challenges are the subject of the present study.

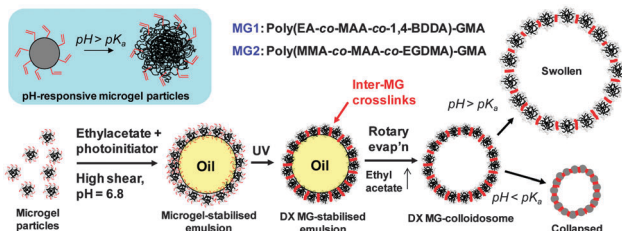
Microgel-colloidosomes are typically prepared *via* the microgel-stabilised emulsion route which uses oil or water droplets as a template.<sup>15,16</sup> This approach benefits from the very high stabilisation afforded to emulsion droplets by adsorbed microgel particles. However, a limitation of previous methods used to prepare microgel-colloidosomes,<sup>11,15,17</sup> and indeed more generally of conventional polymer particle based colloidosomes,<sup>9</sup> is that construction requires two (or more) structure-forming components. Typically a small molecule or polymer-based cross-linking agent is used to link adsorbed particles together at the droplet interface.<sup>11</sup> Approaches using added cross-linkers have the disadvantages of diluting colloidosome stimulus responsiveness and may introduce associated toxicity concerns. We address these problems by using a new assembly approach here.

Recently, we showed that microgel particles which have intra-particle crosslinking could be vinyl-functionalised and covalently inter-linked to give macroscopic three-dimensional hydrogels.<sup>18</sup> The vinyl-functionalised microgels acted as macro-crosslinkers. Those hydrogels consisted only of inter-linked microgel particles and are termed doubly crosslinked microgels (DX MGs). Inspired by a recent report which proposed that microgel particles interpenetrate

School of Materials, The University of Manchester, Grosvenor Street, Manchester, M13 9PL, UK. E-mail: [brian.saunders@manchester.ac.uk](mailto:brian.saunders@manchester.ac.uk)

† Electronic supplementary information (ESI) available: Experimental details and additional characterisation data for the microgels and DX MG-colloidosomes. See DOI: [10.1039/c4cc10169c](https://doi.org/10.1039/c4cc10169c)





**Scheme 1** Illustration of DX MG-colloidosome preparation using pH-responsive microgel particles. The majority of the data presented in this study used MG1 particles. MG2 particles were used to demonstrate versatility.

at oil/water interfaces,<sup>19</sup> we decided to determine whether DX MG-colloidosome preparation could be achieved using covalent inter-linking of adsorbed microgels. Our working hypothesis was that the oil/water interface would promote sufficient microgel deformation and interpenetration to enable covalent inter-linking of peripheral vinyl groups on the microgel particles *via* free-radical coupling. Uniquely, our method for DX MG-colloidosome preparation uses only one type of (colloidal) building block for shell assembly, *i.e.*, the pre-formed microgel particle which acts as a macro-crosslinker. Accordingly, the pH-responsive DX MG-colloidosomes reported here represent a new class of colloidosome.

The method used to prepare our DX MG-colloidosomes is depicted in Scheme 1. The primary pH-responsive vinyl-functionalised microgels used in this study was poly(ethylacrylate-*co*-methacrylic acid-*co*-1,4-butanediol diacrylate)-glycidyl methacrylate (poly(EA-*co*-MAA-*co*-1,4-BDDA)-GMA). The latter (abbreviated as MG1) was prepared by emulsion polymerisation and subsequent reaction with GMA following methods established in our previous work.<sup>18</sup> As a proof of versatility for our DX MG-colloidosome approach we also prepared poly(methyl methacrylate-*co*-methacrylic acid-*co*-ethyleneglycol dimethacrylate)-GMA (poly(MMA-*co*-MAA-*co*-EGDMA)-GMA) microgel (abbreviated as MG2). MG1 and MG2 particles differed considerably in their compositions (Table S1, ESI<sup>†</sup>) because the structural polymer (60–63 mol% of repeat units) was EA or MMA, respectively. Poly(EA) and poly(MMA) are low and high glass transition temperature ( $T_g$ ) polymers, respectively, and have very different mechanical properties.

In our first series of experiments MG1 particles were used to stabilise ethyl acetate-in-water emulsions (Scheme 1) which contained a UV photoinitiator (2-hydroxy-4'--(2-hydroxyethoxy)-2-methylpropiophenone). The role of the photoinitiator was to covalently “stitch together” the MG building blocks at the oil–water interface by free-radical coupling of vinyl groups. After UV irradiation the ethyl acetate was removed by rotatory evaporation at room temperature to give DX MG-colloidosomes. A description of the method used is given in the ESI.<sup>†</sup>

Potentiometric titration data (Fig. S1 and Table S1, ESI<sup>†</sup>) showed that the MG1 particles contained 31.0 mol% MAA and 8.7 mol% of GMA and had a  $pK_a$  of 6.4. The number-average particle size from SEM (Fig. S2a, ESI<sup>†</sup>) was 73 nm (coefficient of variation,  $CV = 12\%$ ). It can be seen from Fig. S2b (ESI<sup>†</sup>) that the MG1 particles showed a strong pH-triggered increase of the hydrodynamic diameter ( $d_h$ ). From those data an estimated volume-swelling ratio at pH = 10 of  $\sim 27$  was calculated using  $Q = (d_{h(\text{pH}=10)}/d_{h(\text{pH}=4.8)})^3$ .<sup>3</sup>

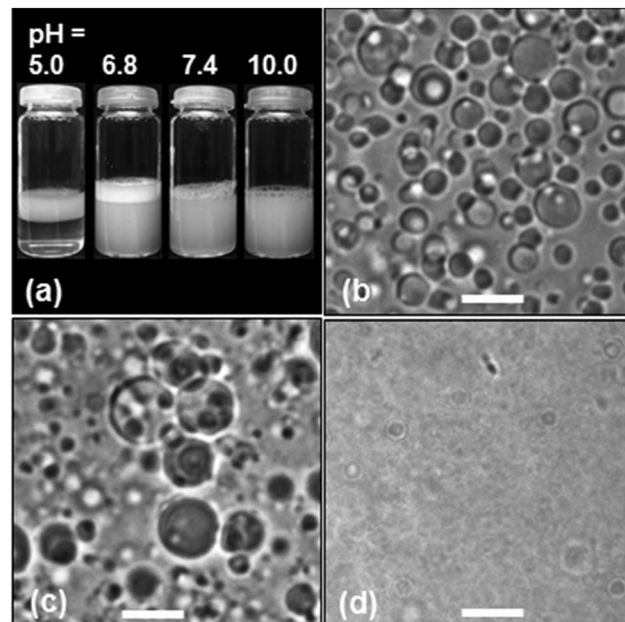


**Fig. 1** Photographs (a) and optical images ((b) to (d)) of microgel-stabilised ethyl acetate-in-water emulsions. The pH values were 6.8 (b), 7.4 (c) and 10.0 (d). Scale bar = 10  $\mu\text{m}$ . The microgel used for this study was MG1.

Addition of the MG1 particles to ethyl acetate and water mixtures followed by high shear resulted in microgel-stabilised oil-in-water emulsions, which are a type of Pickering emulsion. The extent of creaming of the microgel-stabilised emulsions after 10 min was pH-dependent (Fig. 1a). (It should be noted that the white layer at the top of the tubes was foam due to the surface activity of the MG1 particles.) At pH = 5.0 (which corresponds to collapsed microgel particles) the emulsions creamed rapidly and the droplets aggregated. The tendency of microgel-stabilised emulsions to have poor stability when the microgel particles are in the collapsed state has been reported elsewhere.<sup>20</sup> However, at pH = 6.8 the microgel-stabilised droplets were colloidally stable (Fig. 1b) and did not cream over 24 h. The number-average diameter determined from optical microscopy ( $D_{\text{opt}}$ ) for the microgel-stabilised droplets at pH = 6.8 was 3.5  $\mu\text{m}$  ( $CV = 36\%$ ). At pH values greater than or equal to 7.4 the smaller droplets became less visible and at pH = 10 droplets were not able to be visualised clearly by optical microscopy. There was no evidence of phase separation for the tubes at pH values greater than or equal to 6.8. We selected the latter pH for DX MG-colloidosome preparation because it enabled good visualisation of the precursor droplets as well as maximising colloidosome yield.

The morphology of the DX MG-colloidosomes was investigated using complementary microscopy techniques (Fig. 2). Optical micrographs obtained at pH = 6.4 (Fig. 2a and Fig. S3, ESI<sup>†</sup>) revealed the colloidosomes were hollow. The colloidosomes had a  $D_{\text{opt}}$  value of 1.7  $\mu\text{m}$  ( $CV = 22\%$ ). The DX MG-colloidosomes had a significantly smaller size compared to the parent microgel-stabilised emulsion (Fig. 1b) due to removal of the oil phase by rotatory evaporation.

DX MG-colloidosome morphology was probed using CLSM with Rhodamine B labelling (Fig. 2b). Hollow particles were evident (Fig. 2b(i) and (ii)). Sequential z-scanning image profiles were also obtained (Fig. S4, ESI<sup>†</sup>) which revealed that the shell thickness for



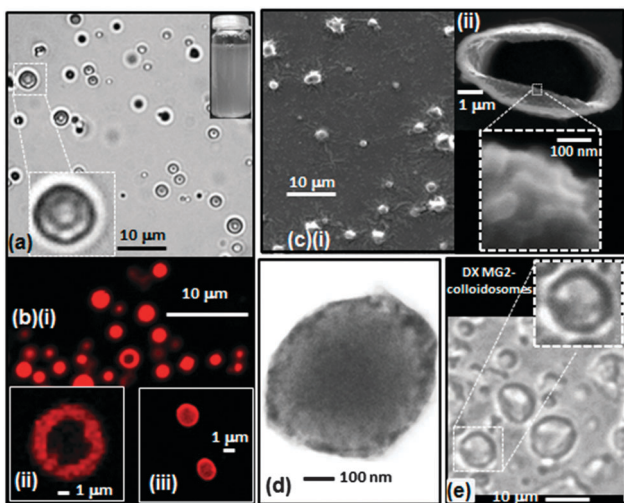


Fig. 2 Optical micrograph and sample vial (a), CLSM images (b), SEM images (c) and a representative TEM image (d) for DX MG-colloidosomes prepared using MG1 particles. (e) Shows an optical micrograph for DX MG-colloidosomes prepared using MG2 particles.

these microgel-colloidosomes was about 1  $\mu\text{m}$ . These images imply that the shells contained multiple layers of microgel particles. Interestingly, decreasing the photoinitiator concentration and using water without added buffer (see Experimental details, ESI<sup>†</sup>) decreased the shell thickness to  $\sim 100$  nm (Fig. 2b(iii)). The pH of these dispersion was  $\sim 6.0$ . The estimated shell thickness of 100 nm is close to the diameter of MG1 particles at this pH ( $\sim 90$  nm, see Fig. S2, ESI<sup>†</sup>). The formulation conditions used to prepare the colloidosomes were analysed (summarised in Table S2, ESI<sup>†</sup>) and show that the mass ratios of photoinitiator to MG ( $\text{MR}_{\text{init/MG}}$ ) used for the high and low initiator concentration DX MG preparations were 0.40 and 0.15, respectively. It can be tentatively proposed from these early-stage results that the shell thickness increases with  $\text{MR}_{\text{init/MG}}$  over the range of 0.1 to 1.0  $\mu\text{m}$  and is tunable. Future work will fully explore the relationship between shell thickness and  $\text{MR}_{\text{init/MG}}$ . All DX MG-colloidosomes discussed in the remainder of this study were prepared using the high photoinitiator concentration method (see ESI<sup>†</sup>) because of the higher yield obtained.

DX MG-colloidosome morphology was also investigated at higher magnification using SEM (Fig. 2c). The colloidosomes were crumpled, due to water removal. A broken colloidosome shows the shell clearly (Fig. 2c(ii)). The expanded image reveals the particulate nature of the shell (inset of Fig. 2c(ii)). Additional high magnification images also clearly showed the presence of microgel particles at the surface (Fig. S5, ESI<sup>†</sup>).

We further probed DX MG colloidosome morphology using TEM (Fig. 2d). A larger extent of electron scattering (and hence microgel) density was evident at the colloidosome periphery, implying a relatively thick shell. Furthermore, TEM of colloidosome clusters (Fig. S6, ESI<sup>†</sup>) showed an elliptical interface (*i.e.*, a “window” structure) between two adjoining colloidosomes confirming their hollow particle nature.

In order to demonstrate the versatility of our DX MG colloidosome preparation method a structurally different, higher  $T_g$ , vinyl-functionalised microgel was used. MG2 (Scheme 1 and Table S1,

ESI<sup>†</sup>) has been used in previous work to prepare biocompatible DX MGs.<sup>21</sup> MG2 particles contained methyl methacrylate as the structural monomer ( $\sim 63$  mol%) and showed strong pH-triggered swelling at pH values greater than 6.2 (Fig. S7a, ESI<sup>†</sup>). DX MG2-colloidosomes were hollow in the as-made state (pH = 6.6) as evidenced by optical microscopy data (Fig. 2e). They had a  $D_{\text{opt}}$  value of 4.0  $\mu\text{m}$  ( $\text{CV} = 34\%$ ). Interestingly, the latter DX MG-colloidosomes had a larger diameter than the colloidosomes prepared using MG1 particles (Fig. 2a). Future work will investigate the origins of this behaviour. These data show that DX MG colloidosomes can be prepared using more than one type of microgel and demonstrate versatility of our method.

There are very few reports of colloidosomes prepared from pH-responsive microgels<sup>10,11</sup> and no studies reported to our knowledge where the colloidosomes are composed exclusively of microgel particles without added structural linkers. For the present DX MG-colloidosomes there were no other components that could interfere with or dilute pH-triggered swelling. Because the MG1 particles exhibited a very strong pH-triggered swelling (Fig. S2b, ESI<sup>†</sup>) the pH-triggered swelling of DX MG-colloidosomes was also investigated. Dynamic light scattering (DLS) data were measured at several pH values (Fig. 3a). As with reports for related systems<sup>7</sup> both colloidosomes and residual microgel particles were present. Importantly, the DX MG-colloidosomes were present at the highest vol% at all pH values studied. A comparison of the areas under the DLS curves for each of the species present in the initial state (pH = 6.4) enabled an estimated conversion efficiency of more than 95% to be calculated. These data imply that only about 5% of the initially dispersed MG1 particles remained in the non-colloidosome state after DX MG colloidosome preparation.

It can be seen from Fig. 3a that the DX MG-colloidosomes showed strong pH-triggered swelling when the pH increased to greater than the  $\text{p}K_{\text{a}}$  of the MG1 particles (6.4). The DX MG colloidosomes detected by DLS were smaller than most of the colloidosomes that could be visualised by optical microscopy and CLSM (Fig. 2a and b), which is expected because the optimal resolutions for our optical microscopy and CLSM measurements were in size range greater than 1  $\mu\text{m}$ . DLS, which is a light scattering technique, is able to detect particles across the length scale of 1 to 10 000 nm and was best suited to studying the smaller colloidosomes. Nevertheless, there was overlap in the diameter ranges probed. For example colloidosomes with a diameter of  $\sim 1.5$   $\mu\text{m}$  that are evident in Fig. 3a match similarly sized colloidosomes that can be seen in the optical micrographs obtained at pH = 6.4 (Fig. S3, ESI<sup>†</sup>).

The calculated volume swelling ratio ( $Q$ ) for the colloidosomes from the DLS data shown in Fig. 3a was  $\sim 50$  using the  $d_h$  values measured at pH values of 6.4 (1440 nm) and 10.0 (5310 nm). Whilst this result is evidence of strong pH-triggered swelling we must exercise caution because it is not certain that the hollow particles were spherical at all pH values. We plan to investigate the relationship between pH and colloidosome shape in future studies.

To further probe the pH-responsiveness of the DX MG colloidosomes an alkaline challenge experiment was conducted. The colloidosome size changes were examined directly using optical microscopy (Fig. 3b and c). In this experiment the pH was increased from 6.4 to 10 by addition of buffer solution to one



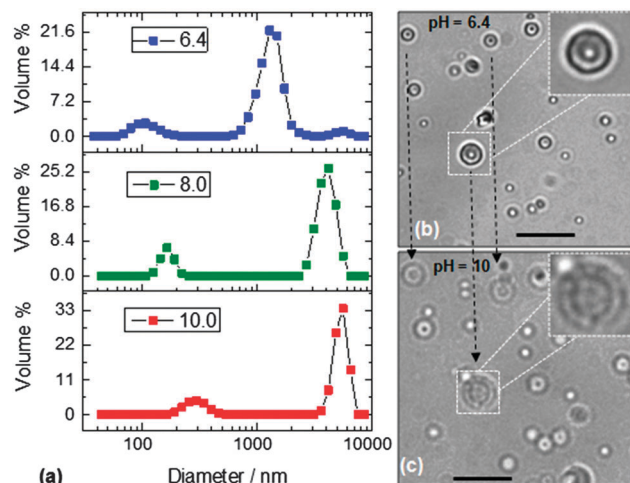


Fig. 3 DLS data measured at various pH values (a) for DX MG-colloidosomes. (b) and (c) show optical micrographs for the colloidosomes at pH = 6.4 and 10, respectively. The arrows show colloidosomes that did not change position when the pH increased. Scale bar = 10  $\mu\text{m}$ . MG1 particles were used for these colloidosomes.

edge of a microscope slide. Several of the colloidosomes had adsorbed onto the slide which, fortuitously, prevented their motion during the experiment. These adsorbed colloidosomes provided an opportunity to directly probe their diameter change with pH. The large colloidosome (insets) in Fig. 3b and c had a diameter of  $\sim 4.0 \mu\text{m}$  at pH = 6.4 and this increased to  $\sim 6.0 \mu\text{m}$  at pH = 10. The relative diameter increase is lower than that observed by DLS, which is most likely due to the immobilisation of the colloidosomes on the microscope slide, which opposed swelling. Nevertheless, the data provide direct confirmation of pH-triggered DX MG-colloidosome swelling. (This pH-triggered swelling was reproducible as can be seen from the two other colloidosome particles in Fig. 3b and c that behaved in a similar way and are joined by dashed lines.) The swelling transition was complete within 2 s which shows that the colloidosomes can respond rapidly to pH increases. Furthermore, the colloidosomes did not fragment or redisperse after swelling.

The DX MG-colloidosomes prepared using the MG2 particles also showed pH-triggered swelling. The  $D_{\text{opt}}$  value for these colloidosomes was  $4.0 \mu\text{m}$  at pH = 6.6 (Fig. 2e) and this increased to  $6.3 \mu\text{m}$  at pH = 12 (Fig. S7b, ESI<sup>†</sup>). It follows that both DX MG-colloidosome types (prepared using MG1 and MG2) exhibited pH-triggered swelling. These observations establish the versatility of our new DX MG-colloidosome preparation method.

The DX MG-colloidosomes did not redisperse when the pH was increased to well above the microgel particle  $pK_a$ . This observation confirms that the microgel particles were covalently inter-linked within an interfacial DX MG hydrogel layer. We tested control colloidosomes prepared from non-vinyl functionalised microgel particles that were not inter-linked. Those colloidosomes spontaneously dispersed when the pH was increased above the  $pK_a$  of the MG1 particles. Consequently, the data help to resolve a discussion in the literature concerning whether or not microgel particle peripheries interpenetrate at oil/water interfaces.<sup>19</sup> Microgel particle peripheral chains do interpenetrate at the oil/water interface and

direct inter-linking of them can occur if the peripheral chains have vinyl groups attached. The latter approach offers potential to construct designer covalent hydrogel network shells around droplets, which can also be transformed into textured responsive hollow capsules and this will be explored in our future work.

In this study we have demonstrated construction of DX MG-colloidosomes for the first time. Moreover, we have shown that our novel approach using vinyl-functionalised microgels as building blocks and macro-crosslinkers is general by using more than one microgel type to prepare DX MG-colloidosomes. The DX MG colloidosomes were prepared using environmentally benign conditions (pH = 6.8) and DX MGs that are biocompatible<sup>21,22</sup> which indicates suitability for incorporation of biological agents in future work. The DX MG-colloidosomes were strongly pH-responsive and exhibited a major pH-triggered swelling response in the physiological pH region which further supports the view that they have good potential for biomaterial applications, which will be explored in future studies. The success of DX MG formation provided novel experimental support for the occurrence of microgel interpenetration at oil/water interfaces and also established a new approach for preparing pH-responsive capsules. Future studies will examine the relationships between microgel structure and DX MG-colloidosome swelling.

## Notes and references

- 1 F. Caruso, R. A. Caruso and H. Mohwald, *Science*, 1998, **282**, 1111–1114.
- 2 O. J. Cayre, J. Hitchcock, M. S. Manga, S. Fincham, A. Simoes, R. A. Williams and S. Biggs, *Soft Matter*, 2012, **8**, 4717–4724.
- 3 H. N. Yow and A. F. Routh, *Soft Matter*, 2006, **2**, 940–949.
- 4 X. Liu, X. Jin and P. X. Ma, *Nat. Mater.*, 2011, **10**, 398–406.
- 5 P. J. Dowding, R. Atkin, B. Vincent and P. Bouillot, *Langmuir*, 2004, **20**, 11374–11379.
- 6 A. N. Zelikin, Q. Li and F. Caruso, *Chem. Mater.*, 2008, **20**, 2655–2661.
- 7 T. Bollhorst, T. Grieb, A. Rosenauer, G. Fuller, M. Maas and K. Rezwan, *Chem. Mater.*, 2013, **25**, 3464–3471.
- 8 O. D. Velev, K. Furusawa and K. Nagayama, *Langmuir*, 1996, **12**, 2374–2384.
- 9 A. D. Dinsmore, M. F. Hsu, M. G. Nikolaides, M. Marquez, A. R. Bausch and D. A. Weitz, *Science*, 2002, **298**, 1006–1009.
- 10 Y. Gong, A. M. Zhu, Q. G. Zhang, M. L. Ye, H. T. Wang and Q. L. Liu, *ACS Appl. Mater. Interfaces*, 2013, **5**, 10682–10689.
- 11 A. J. Morse, J. Madsen, D. J. Gowney, S. P. Armes, P. Mills and R. Szwart, *Langmuir*, 2014, **30**, 12509–12519.
- 12 B. R. Saunders and B. Vincent, *Adv. Colloid Interface Sci.*, 1999, **80**, 1–25.
- 13 C. M. Nolan, M. J. Serpe and L. A. Lyon, *Biomacromolecules*, 2004, **5**, 1940–1946.
- 14 Y. Xia, X. He, M. Cao, X. Wang, Y. Sun, H. He, H. Xu and J. R. Lu, *Biomacromolecules*, 2014, **15**, 4021–4031.
- 15 D. B. Lawrence, T. Cai, Z. Hu, M. Marquez and A. D. Dinsmore, *Langmuir*, 2007, **23**, 395–398.
- 16 Y. Gong, A. M. Zhu, Q. G. Zhang and Q. L. Liu, *RSC Adv.*, 2014, **4**, 9445–9450.
- 17 G. Agrawal, A. Ülpenich, X. Zhu, M. Möller and A. Pich, *Chem. Mater.*, 2014, **26**, 5882–5891.
- 18 R. Liu, A. H. Milani, T. J. Freemont and B. R. Saunders, *Soft Matter*, 2011, **7**, 4696–4704.
- 19 W. Richtering, *Langmuir*, 2012, **28**, 17218–17229.
- 20 M. Destribats, V. Lapeyre, E. Sellier, F. Leal-Calderon, V. Ravaine and V. Schmitt, *Langmuir*, 2012, **28**, 3744–3755.
- 21 A. H. Milani, A. J. Freemont, J. A. Hoyland, D. J. Adlam and B. R. Saunders, *Biomacromolecules*, 2012, **13**, 2793–2801.
- 22 Z. Cui, A. H. Milani, P. J. Greensmith, J. Yan, D. J. Adlam, J. A. Hoyland, I. A. Kinloch, A. J. Freemont and B. R. Saunders, *Langmuir*, 2014, **30**, 13384–13393.

